β-Delayed Deuteron Emission from ^{11}Li: Decay of the Halo

R. Raabe,[1] A. Andreyev,[2] M. J. G. Borge,[3] L. Buchmann,[2] P. Capel,[2] H. O. U. Fynbo,[4] M. Huyse,[1,2] R. Kanungo,[2] T. Kirchner,[2] C. Mattoon,[5] A. C. Morton,[2] I. Mukha,[1,6] J. Pearson,[2] J. Ponsaers,[1] J. J. Ressler,[7,2] K. Riisager,[4] C. Ruiz,[8,2] G. Ruprecht,[2] F. Sarazin,[5] O. Tengblad,[3] P. Van Duppen,[1] and P. Walden[2]

[1]*Instituut voor Kern- en Stralingsfysica, K.U.Leuven, B-3001 Leuven, Belgium*
[2]*TRIUMF, Vancouver, British Columbia, Canada V6T 2A3*
[3]*Instituto de Estructura de la Materia, CSIC, Madrid, Spain*
[4]*Department of Physics and Astronomy, University of Aarhus, DK-8000 Aarhus C, Denmark*
[5]*Department of Physics, Colorado School of Mines, Golden, Colorado 80401, USA*
[6]*Universidad de Sevilla, ES-41080 Seville, Spain*
[7]*Department of Chemistry, Simon Fraser University, Burnaby, B.C. Canada V5A-1S6*
[8]*Department of Physics, Simon Fraser University, Burnaby, B.C. Canada V5A-1S6*

(Received 16 January 2008; published 18 November 2008)

The deuteron-emission channel in the β decay of the halo nucleus ^{11}Li was measured at the Isotope Separator and Accelerator facility at TRIUMF by implanting postaccelerated ^{11}Li ions into a segmented silicon detector. The events of interest were identified by correlating the decays of ^{11}Li with those of the daughter nuclei. This method allowed the energy spectrum of the emitted deuterons to be extracted, free from contributions from other channels, and a precise value for the branching ratio $B_d = 1.30(13) \times 10^{-4}$ to be deduced for $E_{\mathrm{c.m.}} > 200$ keV. The results provide the first unambiguous experimental evidence that the decay takes place essentially in the halo of ^{11}Li and that it proceeds mainly to the ^{9}Li + d continuum, opening up a new means to study the halo wave function of ^{11}Li.

DOI: 10.1103/PhysRevLett.101.212501 PACS numbers: 23.40.Hc, 27.20.+n

The nuclear halo [1] is among the most peculiar features discovered in unstable nuclei. The ^{11}Li nucleus is the showcase of a two-neutron halo system, with its very extended matter distribution related to the small energy necessary to remove the neutrons: $S_{2n} = 378(5)$ keV [2]. Considerable effort has been expended to determine the characteristics of this unstable, short-lived nucleus [$T_{1/2} = 8.5(2)$ ms [3]]. Among the available probes, the β decay has the advantage of being described by a well-established theory and thus provides a valuable tool for the investigation of the properties of the parent nucleus.

In the case of ^{11}Li, the β-delayed deuteron emission $^{11}\mathrm{Li} \xrightarrow{\beta} {}^9\mathrm{Li} + d$ is of special interest. This mode is related to the possibility that in halo nuclei the core and the halo particles could decay, more or less independently, into different channels [4]. Evidence of the β decay of the ^{9}Li core in ^{11}Li with survival of the two-neutron halo was reported in Ref. [5]. On the other hand, according to calculations [6–8] the deuteron-emission channel should be dominated by the decay of a neutron in the halo: a ''halo decay.'' This may be measured via the $^{11}\mathrm{Li} \xrightarrow{\beta} {}^9\mathrm{Li} + d$ decay probability or the branching ratio B_d. In addition, the β-delayed deuteron decay of ^{11}Li could proceed directly to the continuum, without forming an intermediate state (resonance) in the daughter nucleus ^{11}Be. The information on the initial ^{11}Li wave function would then be more easily accessible. Both B_d and the energy distribution of the emitted deuterons are related to this.

We report here the first measurement of the relevant quantities B_d and the energy of the emitted ^{9}Li and d ions, without contributions from other channels, by studying the decay correlations of a postaccelerated ^{11}Li beam implanted in a segmented silicon detector [9,10].

The β decay of ^{11}Li is complex. The large mass difference between ^{11}Li and its daughter ^{11}Be ($Q = 20.6$ MeV) implies that many decay channels to bound and unbound states in ^{11}Be are open. In the latter cases, the daughter breaks into fragments, and emission of one [11], two [12], and three neutrons [13], α particles and ^{6}He [14], tritons [15], and deuterons [16] has been observed. A summary is given in Table I. The β-delayed emission of deuterons has also been observed in the decay of the two-neutron halo nucleus ^{6}He [10,20–22]. However, the $^6\mathrm{He} \xrightarrow{\beta} \alpha + d$ channel has contributions from both the halo and core parts of the ^{6}He ground-state wave function [23–25]; the two contributions interfere destructively leading to a very small value of the corresponding branching ratio of about 10^{-6}. In ^{11}Li, on the other hand, the long-range behavior of the wave function, which is more extended than in ^{6}He, could favor the unperturbed decay of the halo particles and the suppression of the core contribution, producing a comparatively larger branching ratio of the order of 10^{-4} [6–8].

The experimental detection of the deuterons from the $^{11}\mathrm{Li} \xrightarrow{\beta} {}^9\mathrm{Li} + d$ decay is complicated by their low energy—the ^{9}Li + d threshold in ^{11}Be is at $E^* = 17.9$ MeV; thus, the energy available in this channel is $Q_d = 2.7$ MeV. In addition, deuterons are difficult to separate from the tritons emitted in the ^{8}Li + t channel ($Q_t = 4.9$ MeV). The only previous work reporting their detection is that by Mukha *et al.* [16]. The authors measured a cumulative spectrum

TABLE I. β-decay channels of ^{11}Li and decay characteristics of its unstable daughters. Branching ratios for the ^{11}Li channels are estimates from previous works.

	Decay channel		Daughter half-life and decay	
(a)	6.3% [17]	^{11}Be + γ	13.81 s	(1) ^{11}B+γ, 93(1)% [a] (2) Li+α, 7(1)%
(b)	87.6% [17]	^{10}Be + n	10^6 y	
(c)	4.2% [17]	^{9}Be + 2n	Stable	
(d)	1.0% [18]	^{6}He + α + n	807 ms	^{6}Li g.s., $\approx$ 100%
(e)	1.9% [17]	2α + 3n	Stable	
(f)	0.01% [16]	^{8}Li + t	838 ms	2α, 100%
(g)	0.01% [16]	^{9}Li + d	178 ms	(1) ^{9}Be g.s., 49.2(9)% [b] (2) 2α+n, 50.8(9)%

[a]From this work, assuming 6.3(6)% [17] as the branching ratio for (a).
[b]From [19].

for $Z = 1$ particles from the activity of ^{11}Li nuclei deposited on a thin foil and estimated a branching ratio $B \gtrsim 10^{-4}$. Evidence of the actual presence of deuterons was provided by the correlated detection of a few decay events of the associated nucleus ^{9}Li.

In the present work, we used a different experimental technique and directly implanted the ^{11}Li nuclei in a thin, highly segmented silicon detector. The decay channels were identified through the time and position correlation between the implanted nuclei and subsequent parent and daughter decays.

The ^{11}Li nuclei were produced by bombarding a thick Ta target with the 500 MeV, 35 μA proton beam from the TRIUMF Cyclotron. After extraction and selection by a magnetic analyzer, the ^{11}Li nuclei were postaccelerated to an energy of 1.5 MeV/nucleon in the Isotope Separator and Accelerator (ISAC-I) [26]. The implantation into the detector was continuous, at a rate of 200 particles per second (of the total few thousand available) to preserve the correlation between implantation and decay events and reduce the dead time of the acquisition system. The beam was defocused to spread the implantations on the detector surface. About 85×10^6 ^{11}Li ions were implanted in 130 hours of beam time.

The double-sided silicon strip detector was 78 μm thick, with an active area of 16×16 mm^2. The 48 strips on each side (300 μm wide, with those on the back face perpendicular to those on the front) defined a total of 2304 pixels. The efficiency for the detection of low-energy events, measured using pulsed signals of calibrated amplitude, was about 75% at 200 keV, rising to 100% at 300 keV. For all events in each pixel, the recorded information included the deposited energy and a timestamp. The main characteristics of the method have been described in Ref. [10]. A precise normalization is ensured by the direct correlation between implanted ions and detected decays. By selecting single-pixel events (only one signal in each set of strips), β particles are strongly suppressed since their specific energy deposition is low—less than 1% of all β's are detected above the threshold, and fewer than one in 10^6 deposit more than 600 keV [10]. Conversely, the energy deposited by ions in virtually all ^{9}Li + d decay events is completely collected in a single pixel. The range of 1 MeV deuterons in silicon is 12.2 μm, and the interstrip distance was 35 μm. The implantation depth of the ^{11}Li was 43(2) μm according to calculations performed with the code SRIM [27]; this results in 99.9% of the ^{9}Li + d events being contained in the implantation pixel [10].

Figure 1 shows the events immediately following a ^{11}Li implantation in the same pixel. The time behavior has a short component with a half-life $T_{1/2} = 8.7(1)$ ms as expected for ^{11}Li decays. The energy spectrum of events within the first 40 ms—(E_1, t_1) events—contains less than 0.1% background from uncorrelated activity. The features of this ^{11}Li β-decay spectrum will be discussed in a separate publication.

(E_2, t_2) events were defined as the first decay events following the ^{11}Li decays (E_1, t_1) in the same pixel, before a subsequent implantation took place. Such daughter-decay events were used to identify the decay channels of interest (Fig. 2). Referring to Table I, and taking into account that pure β-emission (or $\beta - \gamma$) decays are strongly suppressed in our setup, we expect contributions mainly from the daughters in channels (f) and (g). The

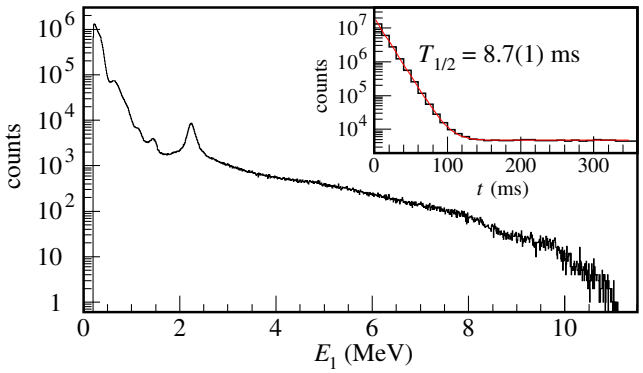

FIG. 1 (color online). Energy spectrum of (E_1, t_1) events, defined as those following a ^{11}Li implantation in the same pixel within 40 ms: These are ^{11}Li decays. The inset shows the time behavior of all events following an implantation: The short-time component has the expected ^{11}Li half-life.

considerably shorter half-life of the ^{8,9}Li daughters compared to the average time between two implantations in the same pixel (about 8.5 s) shows that these daughter decays are truly correlated with the previous ^{11}Li decay. Daughter decays from channel (a) also appear, but they are uncorrelated because their ^{11}Li mother decay branch is mostly not detected (pure $\beta - \gamma$), and due to the long half-life of ^{11}Li. Finally, the spectrum of (E_2, t_2) contains uncorrelated decays of ^{11}Li, due to undetected implantations taking place between the decays at t_1 and t_2. Undetected implantations (caused by the dead time of the acquisition system) are a few percent of the total; still, due to the small branching ratios of the other channels, at low energy the uncorrelated ^{11}Li decays dominate the (E_2, t_2) events.

To correctly evaluate each contribution, the decays of the daughter channels of interest were separately studied in dedicated measurements. Beams of ^{9}Li and ^{8}Li ions were produced at ISAC and implanted with modulations of 0.5 s beam on–0.5 s beam off (^{9}Li) and 2.5 s on–2.5 s off (^{8}Li). For the long-living activity of ^{11}Be we used the ^{11}Li beam with a modulation 20 s on–20 s off. Decay spectra were collected in the beam-off periods; their shapes differed from the ones in literature, reflecting the fact that the sum energy of all emitted ions was measured in our setup (the implantation energies ensured that the ions would not escape). These measurements also allowed us to determine the detection efficiency for each decay: The one for the decay of ^{8}Li was 100(1)% (equal to the branching ratio reported in Table I) because of the high energy of the emitted α particles; for ^{9}Li it was only 36(1)%, resulting from the convolution of the spectrum of the low-energy α particles from the decay with our detection efficiency at energies below 300 keV.

We adopted two procedures to extract the branching ratio and the energy spectrum of the $^{11}\text{Li} \xrightarrow{\beta} {}^{9}\text{Li} + d$ channel. The first consisted of counting the ^{9}Li decays among the (E_2, t_2) events. We fitted the (E_2, t_2) spectrum with the measured spectra of the daughter decays in the channels (a), (f), and (g) (the one of interest) and the spectrum of ^{11}Li decays (from the undetected implantations). The fit was repeated for different time windows Δt (with $t_2 - t_1 < \Delta t$) and various energies E_1 of the first decay; an example is shown in Fig. 2. The asymptotic value of the number of ^{9}Li decays for $\Delta t \to +\infty$ (about 3200 for the whole energy range in E_1), corrected for the detection efficiency, yields the number of deuteron-emission events. An additional small correction was applied to account for the possibility that a subsequent implantation took place in the same pixel before the ^{9}Li decay. By repeating the procedure for different energy intervals in E_1, a differential branching ratio was obtained or, in other words, the decay probability dW/dE as a function of the total $^{9}\text{Li} - d$ energy $E_{\text{c.m.}}$. The result is shown in Fig. 3 (solid circles); the uncertainties (statistical only are plotted) propagate from the errors in the fit of the (E_2, t_2) spectra.

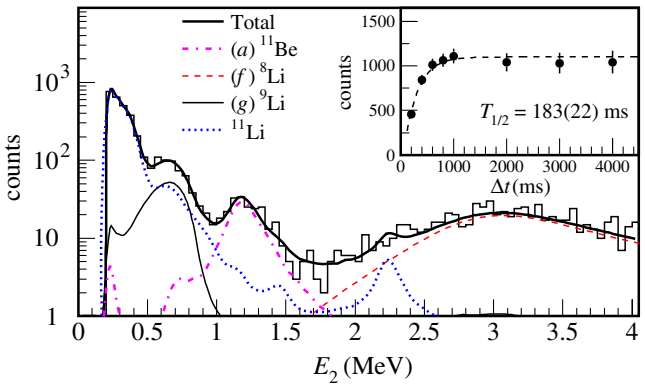

FIG. 2 (color online). Example of a fit of (E_2, t_2) events, with contributions from daughter decays in channels (a), (f), and (g), and uncorrelated ^{11}Li decays. This spectrum was obtained for $t_2 - t_1 < 200$ ms and for E_1 between 0.5 and 2.0 MeV. The inset shows the number of ^{9}Li decay events in the (E_2, t_2) spectra for $t_2 - t_1 < \Delta t$ as function of Δt. The fitted time behavior is in agreement with the expected ^{9}Li half-life $T_{1/2} = 178.3(4)$ ms [19].

The second approach consisted of directly selecting deuteron-emission events among the (E_1, t_1) ones by applying conditions on the subsequent (E_2, t_2) events in order to maximize the number of ^{9}Li decays. This was achieved by requiring $t_2 - t_1 < 200$ ms and E_2 between 0.55 and 0.8 MeV (see also Fig. 2). The amount of "background" present in the selection was determined from the fit of the (E_2, t_2) spectrum; after subtraction, about 700 $^{9}\text{Li} + d$ events remained in the (E_1, t_1) spectrum. The normalization took into account the detection efficiency for the ^{9}Li decay events, plus the factors introduced by the selection of the (E_2, t_2) events. The result is shown in Fig. 3 (hollow squares); because of the smaller statistics, the uncertainties are larger than for the first method.

The two methods produced consistent results within the statistical uncertainties. An additional 8% systematic error is present in both cases, related to the overall normalization. For the total branching ratio of the deuteron-emission channel, the first method (with the better statistics) yields $B_d = 1.30(13) \times 10^{-4}$ for a $^{9}\text{Li} - d$ total energy $E_{\text{c.m.}} > 200$ keV. The value obtained with the second method is $B_d = 1.08(23) \times 10^{-4}$.

B_d is sensitive to two aspects: the decay of the halo part of the ^{11}Li wave function and the decay directly to the continuum rather than to a resonance in the daughter nucleus ^{11}Be. Concerning the first aspect, we have already pointed out how contributions from the core, in the case of ^{6}He, interfere destructively with those from the halo, reducing the branching ratio to about 10^{-6}. As for the second aspect, in the calculations published so far [6–8], it has been shown that a maximum value of $B_d \approx 10^{-4}$ could be reduced (by as much as 2 orders of magnitude) only if a resonance existed below the $^{9}\text{Li} + d$ threshold in ^{11}Be. We conclude that the value which we measured confirms that the deuteron-emission decay takes place essentially in the halo of ^{11}Li, without significant interference from the

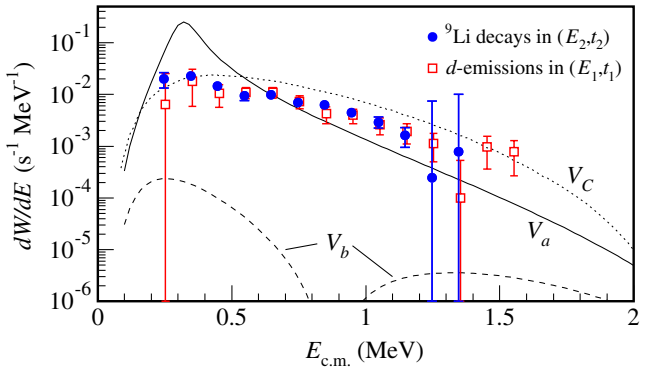

FIG. 3 (color online). Transition probability for the $^{11}\text{Li} \xrightarrow{\beta} {}^9\text{Li} + d$ decay channel. The procedures to obtain the experimental data are explained in the text. The curves are predictions from Refs. [7] (V_C) and [8] (V_a and V_b).

decay of the ^{9}Li core (which was in turn observed in other channels [5]).

The question of whether the decay proceeds directly to the continuum or through a resonance is also related to the energy distribution of the emitted ions (Fig. 3). In Refs. [6–8], different potentials for the $^9\text{Li} - d$ interaction were used to reproduce a resonance around the $^9\text{Li} + d$ threshold in ^{11}Be. The curves in Fig. 3 are taken from those studies and are representative of the results. The curves labeled V_a and V_b (from Ref. [8]) correspond to potentials producing a resonance, respectively, 0.33 MeV above and 0.18 MeV below the $^9\text{Li} + d$ threshold; the one labeled V_C (from Ref. [7]) corresponds to the Coulomb potential only, without a resonance. The integral value of the transition probability rules out the V_b case. A resonance above the threshold, curve V_a, generates a pronounced maximum, shifting the spectrum towards lower energies and reducing it at energies above the resonance; absorption into other decay channels [8] may reduce the height of the maximum but would not affect the spectrum above 1 MeV. This and the fact that our data are better reproduced by the curve V_C indicate that we do not see a resonance in our observation window or just below it. We recall here that a resonance in ^{11}Be has been observed at an excitation energy $E^* \approx 18.1$ MeV by Borge *et al.* [28], about 200 keV above the $^9\text{Li} + d$ threshold. Their analysis, however, based on a branching ratio $B_d \approx 10^{-4}$, showed that it is unlikely that the deuteron-emission decay takes place through this level. Our results thus support the picture of a decay proceeding mainly to the continuum. This implies that the decay matrix elements represent a Fourier transform of the ^{11}Li ground-state wave function to which our data should then be very sensitive. These aspects should be addressed in future theoretical studies.

In conclusion, we have measured the deuteron-emission channel in the β decay of ^{11}Li by implanting a postaccelerated beam of ^{11}Li ions into a highly segmented silicon detector and identifying the channel of interest by the time and position correlation of implantation events and subsequent parent-daughter decays. Precision data were obtained for the branching ratio and the $^9\text{Li} - d$ total energy spectrum down to an energy threshold of 200 keV. The results provide the first clear experimental support for the deuteron-emission decay taking place essentially in the halo of ^{11}Li and indicate that the decay proceeds mainly to the $^9\text{Li} + d$ continuum, opening up the possibility for a detailed study of the halo wave function of ^{11}Li complementary to those based on nuclear reactions.

We thank R. E. Laxdal, P. Bricault, and the operators of the ISAC facility at TRIUMF for their efforts to produce the Li beams. We also thank D. Baye, P. Descouvemont, and M. Zhukov for instructive discussions. This work was supported by the BriX Interuniversity Attraction Poles Programme-Belgian Science Policy (IUAP) under Project No. P6/23 and the Research Foundation-Flanders (FWO), Belgium.

[1] P. G. Hansen, A. S. Jensen, and B. Jonson, Annu. Rev. Nucl. Part. Sci. **45**, 591 (1995).
[2] C. Bachelet *et al.*, Phys. Rev. Lett. **100**, 182501 (2008).
[3] F. Ajzenberg-Selove, Nucl. Phys. **A506**, 1 (1990).
[4] T. Nilsson, G. Nyman, and K. Riisager, Hyperfine Interact. **129**, 67 (2000).
[5] F. Sarazin *et al.*, Phys. Rev. C **70**, 031302(R) (2004).
[6] Y. Ohbayasi and Y. Suzuki, Phys. Lett. B **346**, 223 (1995).
[7] M. V. Zhukov, B. V. Danilin, L. V. Grigorenko, and J. S. Vaagen, Phys. Rev. C **52**, 2461 (1995).
[8] D. Baye, E. M. Tursunov, and P. Descouvemont, Phys. Rev. C **74**, 064302 (2006).
[9] E. S. Paul *et al.*, Phys. Rev. C **51**, 78 (1995).
[10] D. Smirnov *et al.*, Nucl. Instrum. Methods Phys. Res., Sect. A **547**, 480 (2005).
[11] E. Roeckl *et al.*, Phys. Rev. C **10**, 1181 (1974).
[12] R. E. Azuma *et al.*, Phys. Rev. Lett. **43**, 1652 (1979).
[13] R. E. Azuma *et al.*, Phys. Lett. B **96**, 31 (1980).
[14] M. Langevin *et al.*, Nucl. Phys. **A366**, 449 (1981).
[15] M. Langevin *et al.*, Phys. Lett. **146B**, 176 (1984).
[16] I. Mukha *et al.*, Phys. Lett. B **367**, 65 (1996).
[17] M. J. G. Borge *et al.*, Phys. Rev. C **55**, R8 (1997).
[18] S. Landowne and S. C. Pieper, Phys. Rev. C **29**, 1352 (1984).
[19] D. R. Tilley *et al.*, Nucl. Phys. **A745**, 155 (2004).
[20] K. Riisager *et al.*, Phys. Lett. B **235**, 30 (1990).
[21] M. J. G. Borge *et al.*, Nucl. Phys. **A560**, 664 (1993).
[22] D. Anthony *et al.*, Phys. Rev. C **65**, 034310 (2002).
[23] D. Baye, Y. Suzuki, and P. Descouvemont, Prog. Theor. Phys. **91**, 271 (1994).
[24] A. Csótó and D. Baye, Phys. Rev. C **49**, 818 (1994).
[25] E. M. Tursunov, D. Baye, and P. Descouvemont, Phys. Rev. C **73**, 014303 (2006).
[26] *Proceedings of the 14th EMIS Conference*, edited by J. M. D'Auria, J. Thomson, and M. Comyn [Nucl. Instrum. Methods Phys. Res., Sect. B 204, 1 (2003)].
[27] J. F. Ziegler, J. P. Biersack, and U. Littmark, *The Stopping and Range of Ions in Solids* (Pergamon Press, New York, 1985).
[28] M. J. G. Borge *et al.*, Nucl. Phys. **A613**, 199 (1997).